Studies of high energy hadrons in air shower cores at mountain altitude

1974 J. Phys. A: Math. Nucl. Gen. 7 135

(http://iopscience.iop.org/0301-0015/7/1/020)

J. Phys. A: Math., Nucl. Gen., Vol. 7, No. 1, 1974. Printed in Great Britain.

Studies of high energy hadrons in air shower cores at mountain altitude

R van Staa, B Aschenbach† and E Böhm

Institut für Reine und Angewandte Kernphysik der Universität Kiel, Kiel, West Germany

Received 16 July 1973

Abstract. At the Pic du Midi (730 g cm^{-2}) in France an air shower array has been operated to study high energy hadrons in air shower cores. The array consists of 13 scintillation counters of 0·25 m^2 each and a 14 m^2 high energy hadron detector. 2050 showers with a total of 1600 hadrons of energy $E > 100$ GeV have been analysed.

The energy spectrum of hadrons ($E > 300$ GeV) is $H(>E) \sim E^{-\gamma}$ with $\gamma = 1{\cdot}7 \pm 0{\cdot}2$ independent of shower size in the size range $10^5 < N < 10^6$. It is compared with results of different air shower simulations. The lateral distribution can be expressed by $\rho(>E, r) \sim \exp(-r/r_0(>E))$ with $r_0 = 2{\cdot}4(E/200\,\text{GeV})^{-0{\cdot}3\pm0{\cdot}04}$ independent of shower size. It is not necessary to claim for large transverse momenta.

1. Introduction

A primary cosmic ray particle of energy greater than 10^{14} eV falling onto the earth's atmosphere produces a cascade of elementary particles, a so-called extensive air shower (EAS). It consists of hadrons, muons, electrons and photons. Among these particles the high energy hadrons are mainly direct progeny of the primary. Consequently the hadronic component of EAS is closely related to the properties of the incident particle and to the features of the strong interactions, which are responsible for the development of the hadronic cascade:

Therefore studies of high energy hadrons in air shower cores can provide information to answer the following questions:

(i) At energies of around 10^{15} eV there is a break in the primary energy spectrum, which usually is attributed to a rigidity cut-off in our galaxy for primaries of different mass. It is of great interest to check this hypothesis by determination of the chemical composition of the high energy primary cosmic radiation.

(ii) It seems to be well established that the total inelastic cross section and the inelasticity in nucleon–nucleon collisions are constant up to energies of $E_0 = 10^7$ GeV (Trümper 1967), but it has not yet been possible to determine exactly the energy dependence of the multiplicity and to reach agreement about the mean transverse momentum at high energies (Feinberg 1972).

In order to investigate the high energy hadronic component in EAS, a special hadron detector has been used in the Kiel air shower experiment for several years (Bagge *et al* 1965, Fritze *et al* 1970). We have operated similar equipment at mountain altitude for the following reasons:

† Now at Astronomisches Institut der Universität Tübingen, Tübingen, West Germany.

(i) The number of hadrons of fixed energy per shower is increased by one order of magnitude.

(ii) A better determination of the primary energy is possible, since the observed showers are nearer to the maximum of development.

(iii) The similarity of the two equipments provides a good comparison of measurements in two different depths of the atmosphere.

Therefore, at the Pic du Midi (2800 m $\equiv$ 730 g cm^{-2}) in the French Pyrenees we have built up an air shower array with a hadron detector of large area. This work presents results on the integral energy spectrum and the lateral distribution of high energy hadrons in EAS at mountain altitude. Comparing our results with air shower simulations we derive information on multiplicity and mean transverse momentum in high energy collisions. A brief report of our results has been given at the 13th International Cosmic Ray Conference at Denver (van Staa *et al* 1973).

2. Apparatus and methods

The equipment designed in analogy to the Kiel experiment consists of a conventional air shower array and a special hadron detector. Figure 1 shows the air shower array of 13 scintillation counters with an area of 0·25 m^2 each. The four counters on top of the hadron detector serve as triggering devices. The counters 1–4 in addition are equipped with fast timing multipliers. The air shower array enables one to determine arrival direction, core location and size of the recorded showers.

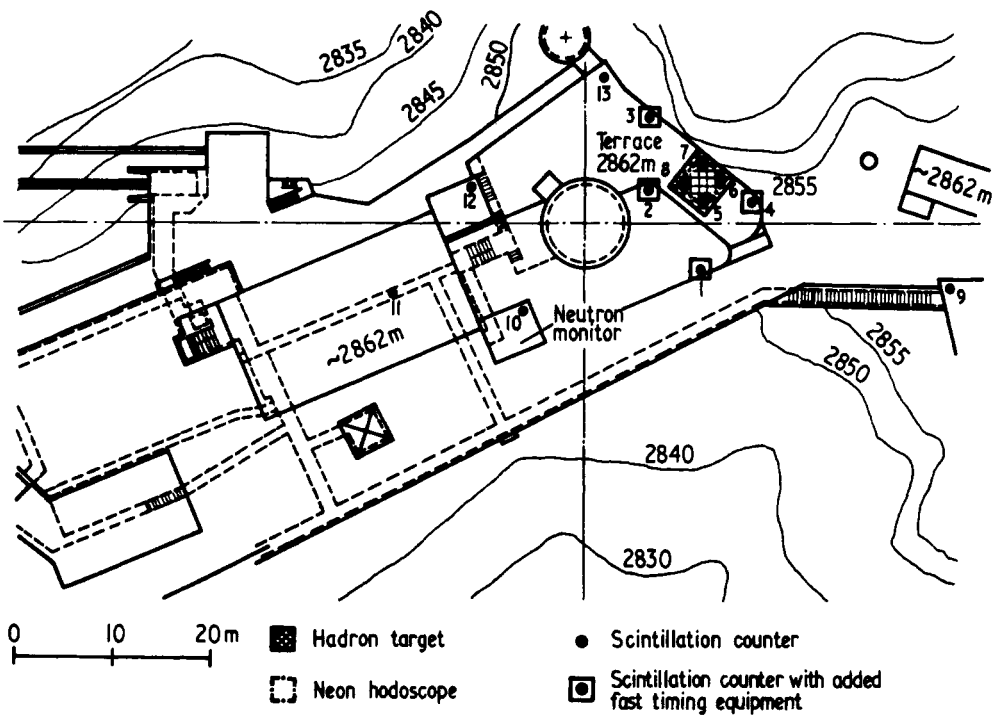

Figure 1. The air shower array at the Pic du Midi.

The hadron detector is shown in figure 2: a layer of 100 cm of sand and 25 cm of concrete serves as a target, in which cascades are produced by high energy hadrons. These cascades can be recognized as bursts in a 14 m^2 neon hodoscope fixed underneath. The hodoscope (Samorski 1973), consisting of about 80 000 neon tubes, has good spatial resolution and provides the coordinates of the individual burst with an error of a few centimetres.

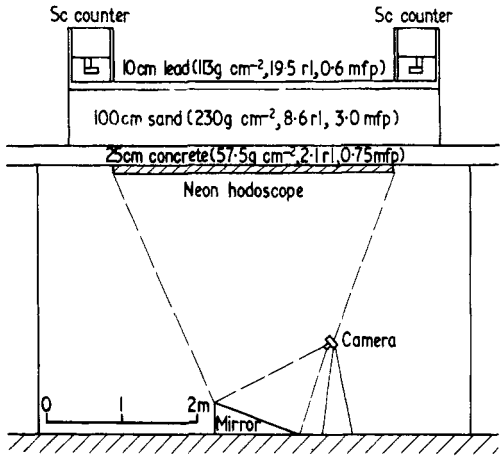

Figure2. The hadron detector.

By measuring the burst size n_b we get information on the energy E of the incident hadron. In order to minimize the error in energy determination the thickness of the target was chosen to be ten radiation lengths (rl), so cascades of 100 GeV hadrons will be observed at the maximum of their development.

On top of the target, in order to absorb the electron–photon component of EAS, there is 10 cm of lead shielding.

3. Results and discussion

2050 showers with a total of 1600 hadrons of energy $E > 100$ GeV have been analysed for the integral energy spectrum and the lateral distribution of hadrons.

3.1. Integral energy spectrum of hadrons

The energy spectrum has to be derived from the number of hadrons, detected in the hodoscope, which is given by

$$G(>E, N) = \int_{F_{NH}} \mathrm{d}F \int_{F(N)} K(N, x, y)\rho(>E, N, x, y)\,\mathrm{d}x\,\mathrm{d}y, \tag{1}$$

where F_{NH} is the hodoscope area, $K(N, x, y)$ is the number of showers with size N, which are recorded per square metre ('shower core density'), $\rho(>E, N, x, y)$ is the lateral distribution of hadrons, and $F(N)$ is the effective area for showers with size N.

Assuming that: (*a*) the linear dimension of the effective area is much larger than the mean distance of hadrons of energy E from the shower axis (this is correct for high energy E and large shower size N); and (*b*) the shower core density is constant for fixed shower size (which is not correct only at the border of the effective area); we can write

$$G(>E, N) = K(N)F_{\mathrm{NH}} \int_0^\infty \rho(>E, N, r)2\pi r \, \mathrm{d}r \tag{2}$$

and obtain the integral spectrum $H(>E, N) = \int_0^\infty \rho(>E, N, r)2\pi r \, \mathrm{d}r$ as

$$H(>E, N) = \frac{G(>E, N)}{K(N)F_{\mathrm{NH}}}. \tag{3}$$

In the following we investigate how errors in the measurement of the hadron energy E, the shower size N and the shower core density $K(N)$ influence the slope of the energy spectrum and the determination of the absolute number of hadrons per shower.

3.1.1. Energy calibration. The hadron energy determination is based on Monte Carlo calculations performed by W V Jones of the Louisiana State University (Jones 1970, private communication), which describe the development of hadron-initiated cascades in concrete. They provide the mean relation between hadron energy E and burst size n_{b}:

$$n_{\mathrm{b}}(E) = kE^{\alpha(t)} \tag{4}$$

where the exponent α is a function of the target thickness t. Our target consists of a layer of 100 cm of sand and 25 cm of concrete, which together corresponds to $t_0 = 10$ rl. With $\alpha(10\ \mathrm{rl}) = 1{\cdot}0$, we get

$$n_{\mathrm{b}} = kE \qquad k = 1\ (\mathrm{particles/GeV}). \tag{5}$$

However, this value of t_0 is not very precise, because the Monte Carlo calculations have been performed for concrete, while we use a layer of sand, the weight of which is not well known in our case. Supposing that t_0 is accurate within 20%, we have a corresponding error in α of $\Delta\alpha = \pm 0{\cdot}08$. For a power law spectrum $H(>E) \sim E^{-\gamma}$ with $\gamma > 1$, this uncertainty in t leads to an error in γ of

$$\Delta\gamma = \pm 0{\cdot}08\gamma. \tag{6}$$

3.1.2. Fluctuations in burst development. The fluctuations in burst development can be expressed by a logarithmic gaussian distribution (Tanahashi 1965). They influence the slope of the measured energy spectra only, if the standard deviation σ of that distribution depends on the hadron energy. The function $\sigma(E)$ can be derived from the Monte Carlo calculations of Jones (see § 3.1.1), which give the mean fluctuations in burst development. For our target the resulting logarithmic standard deviation is

$$\sigma(E = 100\ \mathrm{GeV}) = 0{\cdot}42 \qquad \sigma(E = 1\ \mathrm{TeV}) = 0{\cdot}44. \tag{7}$$

That energy dependence of σ is so weak (since most of the cascades are in, or a little bit behind, the maximum of development, when they reach the hodoscope), that no important change in γ results.

However, the fluctuations in burst development lead to an overestimation of the measured hadron intensity by a factor m (Murzin 1967):

$$m = \exp[\tfrac{1}{2}\sigma^2(\beta - 1)^2], \tag{8}$$

where σ is the standard deviation of the logarithmic gaussian distribution, and β is the exponent of the differential energy spectrum of hadrons.

Supposing the exponent of the integral energy spectrum of hadrons to be $\gamma = 1{\cdot}7$, as derived as an experimental result in § 3.1.6, we get $\beta = 2{\cdot}7$ and $m = 1{\cdot}2$.

3.1.3. Absorber. With a probability of about 50% the first interaction of the hadron happens in the lead absorber. In order to estimate the resulting influence on the energy calibration, given in equation (5), a rough model has been used.

If a hadron interacts the first time in lead, it transfers the energy $K_\gamma E$ ($K_\gamma \simeq 0{\cdot}2$) into a 'lead cascade'. In the hodoscope this electromagnetic cascade provides a burst of size n_1, which we can calculate using cascade curves (Rossi 1952) and taking into account the transition effect (Pinkau 1965). The next interactions of the hadron happen in sand, where they initiate a cascade with burst size $n_2 = (1 - K_\gamma)E$ (see equation (5)). The total burst size detected in the hodoscope is $n = n_1 + n_2$.

If the first hadron interaction happens in the sand we take the energy calibration of equation (5). Then the new conversion factor k is given by

$$k = \frac{\int n(x)W(x)\,\mathrm{d}x}{E} \tag{9}$$

where $W(x)$ is the probability that the first interaction happens in the depth x. In the range $300\ \mathrm{GeV} \leqslant E \leqslant 5\ \mathrm{TeV}$ we get values of k between 0·90 and 0·96.

The reason for the small change in k is the fact that (because of the transition effect) $n_1 \simeq 0$ in the case of interactions near the top of the absorber and $n_1 > (E/1\ \mathrm{GeV}) - n_2$ in the case of collisions at the lower border of the absorber. The fluctuations, which are produced additionally by hadron interactions in lead, should be smaller than K_γ. Therefore they are negligible compared with those of § 3.1.2.

3.1.4. Non-hadronic particles. In the layer of lead and sand high energy muons, electrons and photons can produce cascades, which we are not able to distinguish from 'hadronic' bursts in the individual event.

With respect to the transition effect one can estimate that an electron needs an energy of about 10 TeV to initiate a cascade with burst size $n_{\min} = 100$, which is the lower limit of the observed burst size range. Extrapolating the integral energy spectrum of the electron–photon component of EAS (Toyoda 1962) we find the number of electrons and photons with $E \geqslant 10\ \mathrm{TeV}$:

$$H_{\mathrm{EP}}(E \geqslant 10\ \mathrm{TeV}) = 0{\cdot}06\frac{N}{10^5}\ (\mathrm{particles/shower}) \tag{10}$$

which is less than the number of hadrons of energy $E \geqslant 100\ \mathrm{GeV}$ by a factor of the order 10^{-2}.

The number of muon initiated bursts n_μ can be estimated in comparison with measurements performed at the Kiel air shower experiment (Fritze *et al* 1970), where a ratio $n_\mu/n_{\mathrm{H}} = 0{\cdot}16$ has been found for a lower limit of hadron energy $E_{\min} = 1{\cdot}5\ \mathrm{TeV}$. This value should be considerably smaller in the Pic experiment because of two reasons:

(i) At mountain altitude the number of hadrons per shower is greater by one order of magnitude, while the muon intensity does not change significantly.

(ii) The lower limit of recorded hadron energies is smaller: $E_{\min} = 100\ \mathrm{GeV}$.

3.1.5. Determination of shower size and core location. We have investigated the influence of the configuration of our apparatus on the determination of shower size and core location by simulating the incidence of showers with given size N_0, given lateral distribution of shower particles and random core location (x_0, y_0). The exact particle density ρ_i in each of the scintillation counters has been calculated. By means of the Monte Carlo method poissonian density fluctuations $\Delta\rho_i$ have been added. These artificial showers have been analysed like real shower data.

Comparing the resulting values N and (x, y) with N_0 and (x_0, y_0) respectively, we come to the following conclusions:

(i) Near the trigger level of our apparatus ($N = 10^5$) the shower size is overestimated by a factor 3.

(ii) Cores of showers near to the hodoscope are shifted to the centre, while the other ones are analysed to be at a greater distance from the centre. This effect becomes significant for $N_0 \geqslant 10^6$.

(iii) Correlated with effect (ii) there is a bias of the calculated shower size. A shift of the calculated core location to the centre leads to an underestimation of the shower size and vice versa. So the mean calculated size $\bar{N}$ of showers, which hit the centre of the apparatus, is less than the given size N_0: $\bar{N} < N_0$, while the value $\bar{N}$ of showers with core location within a distance of several metres from the hodoscope is greater than N_0: $\bar{N} > N_0$.

The consequence of (i) is an overestimation of the primary energy by a factor of about 3 in the range $10^5 \leqslant N \leqslant 10^6$. The effects (ii) and (iii) cause an uncertainty of the shower density of about 30%. In addition they give rise to a steepening of the integral energy spectrum of hadrons with increasing shower size, since the mean distance of the hadrons from the shower axis is a function of hadron energy. The fact that the slope of the hadron energy spectrum is independent of shower size has been confirmed by introducing instead of the shower size N a new parameter z, which is the mean particle density detected in the counters 5–8. On the average z depends linearly on the real shower size N_0, but is not influenced by any computational method. So if there is any shower size dependence of the slope of the energy spectrum, it must be found as a dependence of the steepness of the spectra $H(>E, z)$ on z. The result of our analysis is that the slope of H is really independent of z.

3.1.6. The experimental integral energy spectrum of hadrons. Disregarding showers with size $N \geqslant 10^6$ (with respect to effect (iii) of § 3.1.5) we can give the integral energy spectra of hadrons in the range $10^{5.1} \leqslant N \leqslant 10^{5.9}$ (figure 3). Above $E = 300$ GeV they can be expressed by a power law:

$$H(>E, N) = A\left(\frac{N}{N_0}\right)^{\beta}\left(\frac{E}{1\ \text{TeV}}\right)^{-\gamma} \qquad \text{(hadrons/shower)} \tag{11}$$

$$A = 1{\cdot}0 \pm 0{\cdot}3, \qquad N_0 = 3 \times 10^5$$

$$\beta = 0{\cdot}9 \pm 0{\cdot}2, \qquad \gamma = 1{\cdot}70 \pm 0{\cdot}15$$

where the error limits are consequences of the effects discussed in §§ 3.1.1–3.1.5.

In figure 4 our integral energy spectrum for a shower size range $3 \times 10^5 \leqslant N \leqslant 10^6$ is compared with spectra which have been measured at Mt Chacaltaya (Hasegawa *et al* 1965), Mt Norikura (Miyake *et al* 1970, Yoshii 1971), Mt Ootacamund (I: Chatterjee *et al* 1968, II: Sreekantan 1971) and Mt Pamir (Dovzenko *et al* 1959). There is good agreement with the Norikura spectrum, while the other distributions are too flat (Pamir,

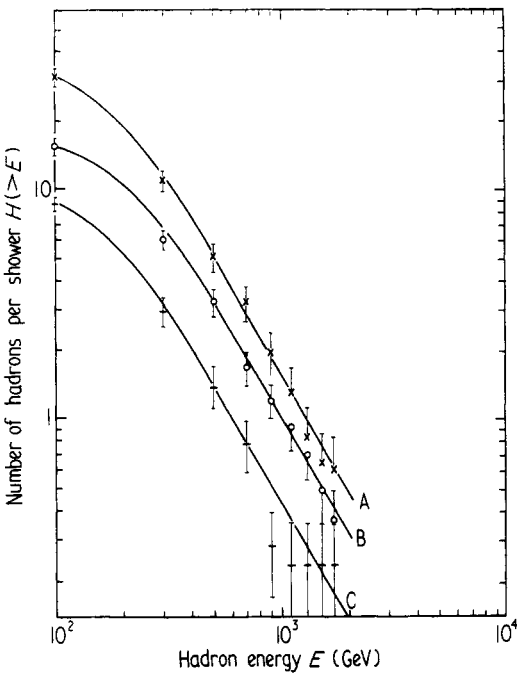

Figure 3. Integral energy spectra of hadrons for different shower sizes. A, $5{\cdot}7 \leqslant \lg N \leqslant 5{\cdot}9$; B, $5{\cdot}4 \leqslant \lg N \leqslant 5{\cdot}6$; C, $5{\cdot}1 \leqslant \lg N \leqslant 5{\cdot}3$.

Chacaltaya, Ootacamund I) or too steep (Ootacamund II) from our point of view. Moreover, the author of Ootacamund II finds a shower size dependent slope of the energy spectra in the range $10^5 \leqslant N \leqslant 3 \times 10^5$, which cannot be confirmed by our results. From our point of view there are three important problems of measurement causing the differences, which become obvious in figure 4: (*a*) accuracy in the determination of the hadron energy; (*b*) spatial resolution of the hadron detector; (*c*) specific properties of the air shower array (see § 3.1.5).

3.1.7. Comparison with air shower simulations. With special regard to the slope we have compared our energy spectrum with computer simulations of air showers. Bradt and Rappaport (1967) and Thielheim and Beiersdorf (1969) have performed Monte Carlo calculations for sea level, which are based on a multiplicity law $n \sim E^{\beta}$ ($\beta \simeq 0{\cdot}25$). The resulting energy spectra are represented by power laws with an exponent $\gamma \simeq 1{\cdot}2$ in the energy range $100\,\text{GeV} \leqslant E \leqslant 2\,\text{TeV}$. They are significantly flatter than our experimental result.

A direct comparison with Monte Carlo calculations for the same observation level is shown in figure 5. The models SFB ($n \sim E^{1/2}$) and IDFB ($n \sim E^{3/8}$) computed by Grieder (1972, private communication) and the model HL ($n \sim E^{1/2}$) of Murthy *et al* (1968) lead to a good agreement of the slope with our measurement, while the model DFB ($n \sim E^{1/4}$) of Grieder and the other models of Murthy (not shown in this figure) produce spectra which are not steep enough from our point of view.

All these Monte Carlo calculations are performed for protons as primary particles. A mean atomic weight of the primaries $\bar{A} > 1$ steepens the energy spectrum of hadrons. The amount of steepening can be estimated from the calculations of Thielheim and

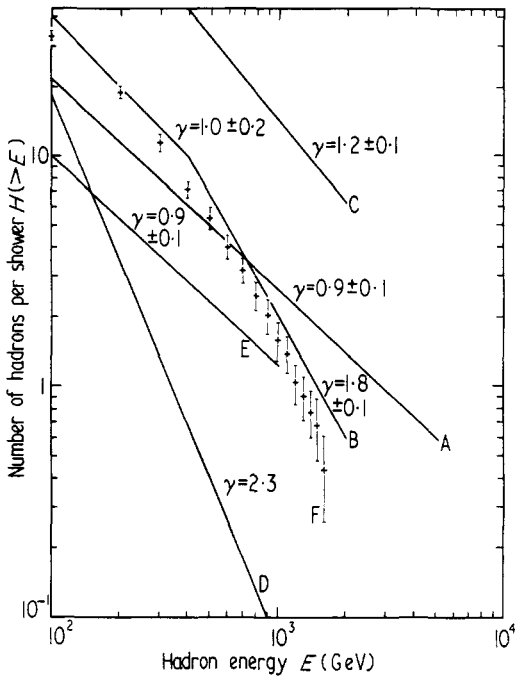

Figure 4. Comparison of the integral energy spectrum of hadrons with other experiments (for references see text). A, Chacaltaya (5200 m), $3 \times 10^5 \leqslant N \leqslant 9 \times 10^5$; B, Norikura (2800 m), $3 \times 10^5 \leqslant N \leqslant 10^6$; C, Ootacamund I (2200 m), $3 \times 10^5 \leqslant N \leqslant 6 \times 10^5$; D, Ootacamund II (2200 m), $3{\cdot}2 \times 10^5 \leqslant N \leqslant 5{\cdot}6 \times 10^5$; E, Pamir (3500 m), $N = 10^5$; F, Pic du Midi (2800 m), $3 \times 10^5 \leqslant N \leqslant 10^6$.

Beiersdorf (1969): an increase from $A = 1$ to $A = 64$ is correlated with a rise of the mean slope of the integral hadron energy spectrum from $\gamma = 1{\cdot}2$ to $\gamma = 1{\cdot}35$ in the energy range 100 GeV $\leqslant E \leqslant$ 10 TeV. This seems to indicate that even a pure heavy particle composition would not be able to explain the steepness of the measured energy spectrum.

The experimental spectrum corresponds to a primary energy $E_0 = (3 \pm 1) \times 10^5$ GeV, assuming the relation $E_0 = 2N$ (GeV) between shower size N and energy E_0. In spite of the uncertainty, which is involved in this relation, our distribution seems to favour the model IDFB, if in addition we take into account the absolute intensity.

Summarizing these arguments, we conclude that a comparison of the measured integral energy spectrum with the above considered Monte Carlo calculations at fixed primary energy indicates that the mean multiplicity in high energy collisions increases more rapidly than $E^{1/4}$ (supposing that the inelastic cross section and the inelasticity are not significantly dependent on collision energy).

On the other hand, calculations performed by Capdevielle (1972), using the 'step-by-step' method, lead to an integral energy spectrum

$$H_c(>E, N) \sim N^{1{\cdot}07} E^{-1{\cdot}7} \qquad (E > 300\,\text{GeV}) \tag{12}$$

in good agreement with our measurement, although based on a quarter law of the mean multiplicity. Apparently there is a difference between the results derived by Capdevielle and by the authors of the Monte Carlo calculations. One possible explanation could be that the first one is presenting his energy spectrum at fixed shower size, while the other ones give spectra at fixed primary energy. Furthermore it is to be noted

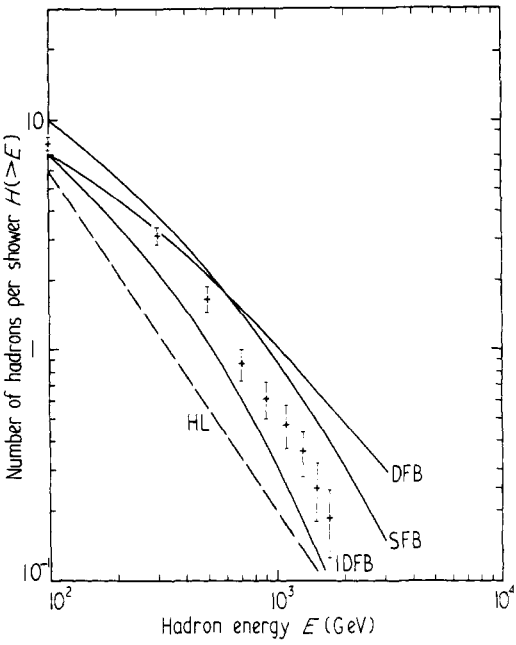

Figure 5. Comparison of the integral energy spectrum of hadrons with Monte Carlo calculations. Full curves: Grieder (1972, private communication), $E_0 = 10^5$ GeV (720 g cm^{-2}); broken curve: Murthy *et al* (1968), $E_0 = 10^5$ GeV (800 g cm^{-2}); experimental points: present work, $E_0 = (3 \pm 1) \times 10^5$ GeV (730 g cm^{-2}).

that in the calculations of Capdevielle fluctuations are allowed only for the first interaction. This may lead to an underestimation of the probability of a hadron reaching the observation level with rather high energy, and therefore it may result in a steepening of the integral energy spectrum.

Nevertheless the conclusion we have drawn concerning the mean multiplicity must be somewhat restricted, until the differences between the results of both methods of air shower simulation are completely clarified.

3.2. Lateral distribution of hadrons

In order to get the lateral distribution of hadrons we have subdivided the neon hodoscope into 100 subareas of 0·14 m^2 each, which can be interpreted as individual burst detectors. Then the lateral distribution is given by

$$\rho(>E, N, r) = \frac{\sum_{i=1}^{100} b_i(>E, N, r)}{\sum_{i=1}^{100} m_i(N, r)} \frac{1}{0{\cdot}14\ \mathrm{m}^2} \tag{13}$$

where $b_i(>E, N, r)$ is the number of showers with size N, incident at a distance r from the ith detector, which are accompanied by a hadron of energy greater than E recorded in the ith detector. $m_i(N, r)$ is the number of all showers with size N falling in at the distance r from the ith detector.

Figure 6 shows the lateral distribution of hadrons for a shower size range $10^{5\cdot1} \leqslant N \leqslant 10^{6\cdot5}$. It can be expressed by an exponential law:

$$\rho(>E, r) = A(>E) \exp(-r/r_0(>E)). \tag{14}$$

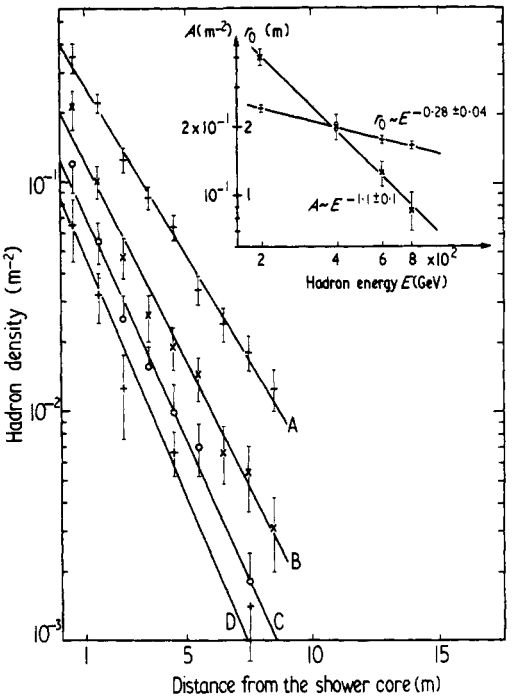

Figure 6. Lateral distributions of hadrons for different hadron energies, and energy dependence of the parameters A and r_0 in the shower size range $5{\cdot}1 \leqslant \lg N \leqslant 6{\cdot}5$. A, $E > 200$ GeV ($r_0 = 2{\cdot}40$ m); B, $E > 400$ GeV ($r_0 = 2{\cdot}00$ m); C, $E > 600$ GeV ($r_0 = 1{\cdot}75$ m); D, $E > 800$ GeV ($r_0 = 1{\cdot}65$ m).

The energy dependences of r_0 and A are given by power laws:

$$r_0(>E) \sim E^{-0{\cdot}3 \pm 0{\cdot}04}, \qquad A(>E) \sim E^{-1{\cdot}1 \pm 0{\cdot}1}. \tag{15}$$

Integration of the lateral distribution leads to the integral energy spectrum:

$$H(>E) = \int_0^\infty \rho(>E, r) 2\pi r \, \mathrm{d}r = 2\pi A(>E) r_0^2(>E) \sim E^{-1{\cdot}7} \tag{16}$$

in agreement with our results in § 3.1.6. Figure 7 shows the lateral distribution of hadrons with $E > 200$ GeV for different shower sizes. It can be seen that r_0 is independent of shower size.

In figure 8 we compare our lateral distribution with results of the experiments at Mt Chacaltaya, Mt Norikura and Mt Ootacamund (for references see § 3.1.6). There is fairly good agreement with the Norikura spectrum. Moreover, the dependences of the parameters A and r_0 on hadron energy E and shower size N agree with those observed at Mt Norikura, with one exception: Miyake *et al* (1970) find that the mean distance of hadrons from the shower axis is a function of shower size: $r \sim N^{0{\cdot}16}$, while our experiment does not show such a dependence. The other distributions are too flat from our point of view.

3.2.1. Errors in determination of the mean distance of hadrons. In order to estimate the mean transverse momentum in high energy collisions by means of the mean distance

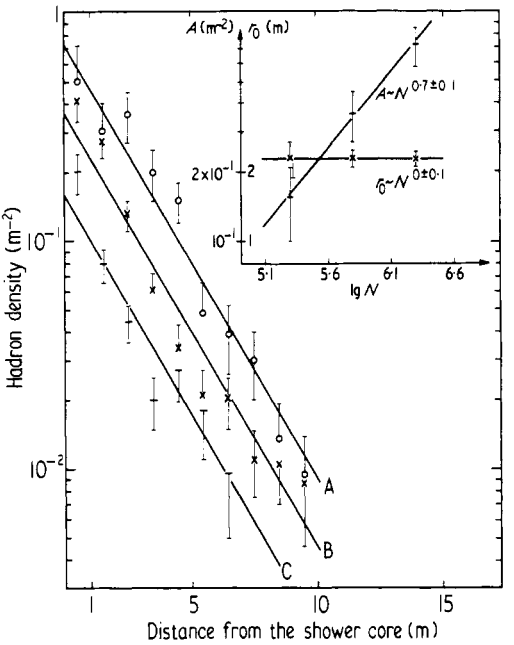

Figure 7. Lateral distributions of hadrons with energy $E > 200$ GeV for different shower sizes, and shower size dependence of the parameters A and r_0. A, $10^{6\cdot1} \leqslant N \leqslant 10^{6\cdot5}$ ($r_0 = 2{\cdot}3$ m); B, $10^{5\cdot6} \leqslant N \leqslant 10^{6\cdot0}$ ($r_0 = 2{\cdot}3$ m); C, $10^{5\cdot1} \leqslant N \leqslant 10^{5\cdot5}$ ($r_0 = 2{\cdot}3$ m).

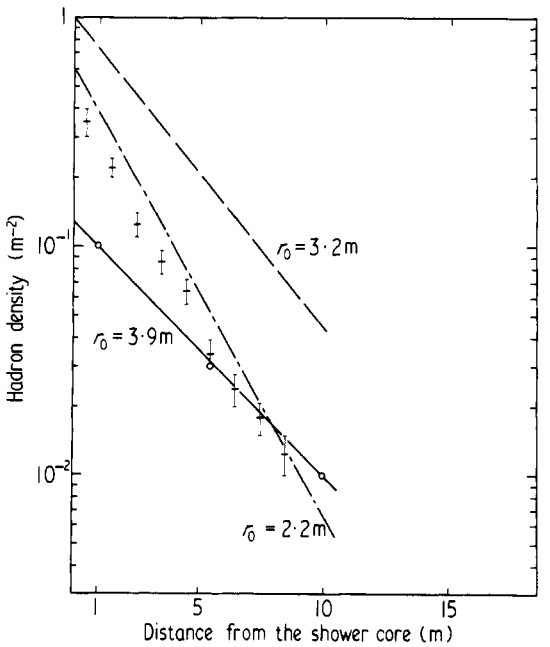

Figure 8. Comparison of the lateral distribution of hadrons with other experiments (for references see text). Full line, Chacaltaya, $250 \leqslant E \leqslant 750$ (GeV), $N = 5 \times 10^5$; chain line, Norikura, $E > 200$ GeV, $3 \times 10^5 \leqslant N < 10^6$; broken line, Ootacamund I, $E > 200$ GeV, $1{\cdot}8 \times 10^5 \leqslant N \leqslant 3{\cdot}2 \times 10^5$; experimental points, Pic du Midi, $E > 200$ GeV, $10^{5\cdot1} \leqslant N \leqslant 10^{6\cdot5}$.

$\bar{r}$ of hadrons from the shower axis, it is useful to consider the influence of our apparatus on the determination of $\bar{r}$. In our measurements we find two main origins, which both produce a flattening of the measured lateral distribution.

(*a*) *Determination of hadron energy.* In principle the measurement of an energy dependent parameter p is influenced by the energy spectrum, the error in energy determination and the energy dependence of p itself.

In the case of the mean distance $\bar{r}(E)$ of hadrons from the shower axis, the steepness of the hadron energy spectrum and the fluctuations in cascade development (see § 3.1.2) lead to an overestimation of $\bar{r}(E)$, because $\bar{r}$ is connected to a measured hadron energy, which is greater than the real energy, and because $\bar{r}$ increases with decreasing energy. Quantitatively, the mean distance of hadrons is increased by a factor (Murzin 1967)

$$b = \exp\{-\tfrac{1}{2}\sigma^2[2(\beta-1)s-s^2]\}, \tag{17}$$

where β is the exponent of the differential energy spectrum of hadrons, σ is the standard deviation of the logarithmic gaussian distribution describing the fluctuations in cascade development (see § 3.1.2), and s is the exponent of the power law, giving the differential energy dependence of the mean distance of hadrons from the shower axis (see equations (20) and (24)).

(*b*) *Determination of the hadron–shower axis distance.* Since the spatial resolution of the neon hodoscope is good, the uncertainty in the determination of the hadron–shower axis distance is identical with the error in the shower core location. By means of the Monte Carlo calculations, described in § 3.1.5, we found that this error Δr is given by

$$H(\Delta r) \sim \Delta r \exp[-(\Delta r)^2/2\sigma_r^2] \tag{18}$$

where σ_r is increasing with the distance R of the given shower core location from the centre of the apparatus:

$$\sigma_r(R) = \exp(0{\cdot}06R). \tag{19}$$

This dependence of the error in shower core location on R leads to a flattening of the lateral distribution of hadrons, causing an increase of the mean distance of hadrons by an additive term of at least 0·3 m, which is a lower limit.

3.2.2. Estimation of the mean transverse momentum. Taking into account the effects discussed above we can estimate the mean transverse momentum. The Monte Carlo calculation performed by Bradt and Rappaport (1967), which is based on a mean transverse momentum $\bar{p}_t = 0{\cdot}35$ GeV/c, leads to a lateral distribution of hadrons which is shown in figure 9 together with the experimental distribution. In the energy range 230 GeV $\leqslant E \leqslant$ 750 GeV the resulting mean distance of hadrons from the shower axis is $\bar{r}_{BR} = 2{\cdot}7$ m, depending on energy as

$$\bar{r}(E) \sim E^s, \qquad s = -0{\cdot}6. \tag{20}$$

Starting from these theoretical values we can calculate formula (17) with $\beta = 2{\cdot}7$, $\sigma = 0{\cdot}43$, $s = -0{\cdot}6$ and we find $b = 1{\cdot}25$. Therefore regarding the two effects (*a*) and (*b*) we expect for the measured mean distance of hadrons:

$$\bar{r}' \geqslant 1{\cdot}25\bar{r}_{BR} + 0{\cdot}3\text{ m} = 3{\cdot}7\text{ m} \tag{21}$$

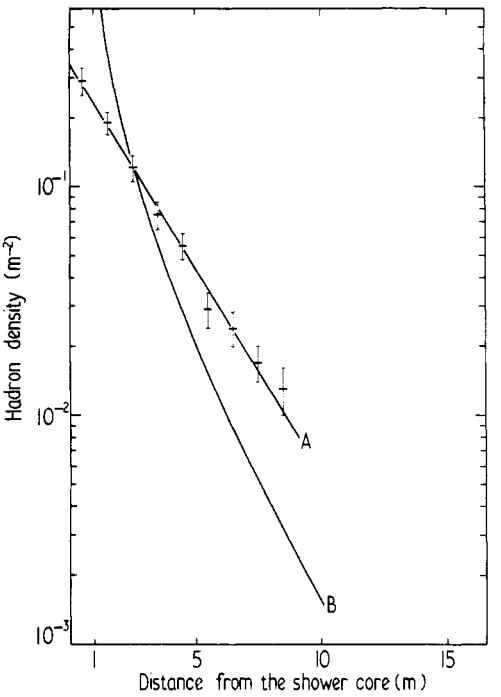

Figure 9. Comparison of the lateral distribution of hadrons with a Monte Carlo calculation of Bradt and Rappaport (1967). A, present work, $E_0 = 8 \times 10^5$ GeV, 730 g cm^{-2}, $200 \leqslant E \leqslant 800$ (GeV), $\bar{r} = 5{\cdot}0$ m; B, Bradt and Rappaport (1967), $E_0 = 10^6$ GeV, 530 g cm^{-2}, $230 \leqslant E \leqslant 750$ (GeV), $\rho_{BR}(r)\,dr = A \exp[-(r/0{\cdot}135\text{ m})^{1/2}]\,dr$, $\bar{r} = 2{\cdot}7$ m.

as a lower limit. So we find a ratio of the experimental value $\bar{r}_{ex} = 5{\cdot}0$ m to the expected value $\bar{r}'$:

$$\bar{r}_{ex}/\bar{r}' \leqslant 1{\cdot}35 \tag{22}$$

which leads to an upper limit of the mean transverse momentum

$$\bar{p}_t = 0{\cdot}47\ \text{GeV}/c. \tag{23}$$

If we consider the differential energy dependence of the mean distance of hadrons, resulting from the experiment:

$$\bar{r}(E) \sim E^{s'}, \qquad s' \simeq -0{\cdot}3 \tag{24}$$

(which is nearly the same as the integral energy dependence (equation (15)), because of the steepness of the hadron energy spectrum), we get with formula (17): $b = 1{\cdot}12$, and the upper limit of the mean transverse momentum becomes

$$\bar{p}_t = 0{\cdot}53\ \text{GeV}/c. \tag{25}$$

The theoretical value of the mean distance of hadrons is the result of a calculation for a pure proton composition of the primary radiation. For a mixed chemical composition, the theoretical lateral distribution of hadrons flattens (Bradt and Rappaport 1967), and

our upper limit of the mean transverse momentum approaches the value $\bar{p}_t = 0{\cdot}35\ \mathrm{GeV}/c$. Therefore, we conclude that it is not necessary to claim for large mean transverse momenta.

4. Conclusions

In the hadron energy range $300\ \mathrm{GeV} \leqslant E \leqslant 2\ \mathrm{TeV}$ the integral energy spectrum, expressed by a power law, has a slope of $1{\cdot}70 \pm 0{\cdot}15$ independent of shower size in the size range $10^5 \leqslant N \leqslant 10^6$. As shown in § 3.1 the steepness of the measured spectrum can be influenced seriously by the method of energy determination and by the uncertainties in shower size and core location. These effects may explain the discrepancy of the results of different experiments shown in figure 4.

The steepness of the measured integral energy spectrum disagrees with the results of all Monte Carlo calculations we have considered, which are based on a multiplicity law $n \sim E^{1/4}$. This discrepancy cannot be explained by the assumption of a heavy primary particle composition. The satisfactory agreement with the models IDFB and DFB of Grieder (1972, private communication) allows the suggestion that the mean multiplicity in high energy collisions increases more rapidly than $E^{1/4}$. This conclusion is restricted to the comparison with the Monte Carlo calculations we have considered, since the results of the 'step-by-step' calculations of Capdevielle (1972) do not permit such a statement.

The mean distance of hadrons from the shower axis increases as $E^{0{\cdot}3}$ for hadron energies of $E > 200\ \mathrm{GeV}$ up to $E > 800\ \mathrm{GeV}$. It is independent of shower size in the range $10^5 < N < 10^{6{\cdot}5}$ for hadrons of energy $E > 200\ \mathrm{GeV}$. The fluctuations in burst development and the error in the determination of the shower core both cause an overestimation of the mean distance of hadrons. The quantitative determination of the extent of these effects, as performed in § 3.2, leads to a mean transverse momentum in high energy collisions of $\bar{p}_t = 0{\cdot}5\ \mathrm{GeV}/c$, which is an upper limit.

During the analysis of the data to this work, it became obvious to the authors that systematical influences of the apparatus on the results of measurement can become very important. So it seems very desirable that the Monte Carlo method should be applied not only to the air shower development, but also to the method of measurement.

Moreover, to get a better comparison between simulations and experiment, it would be helpful to have more calculations with results given at a fixed shower size, or to have better information on the relation between fixed observed shower size and mean correlated primary energy, instead of the relation between fixed primary energy and mean correlated shower size which is usually given.

Acknowledgments

The authors are very grateful to Professor E Bagge for his encouragement. They would like to express their sincere thanks for continuous interest and valuable discussions to Professor J Trümper (now at University of Tübingen, Germany), who has initiated this experiment and has taken part in the first stage of development.

They are indebted to Professor W V Jones (Baton Rouge, USA) and Dr P K F Grieder (Bern, Switzerland), who made the results of their Monte Carlo calculations available to the authors. They wish to thank Dr A Cachon (Bagnères de Bigorre, France) for all his help during their work at the Pic du Midi.

This work has been supported by the Deutsche Forschungsgemeinschaft under grant Tr 11/6.

References

Bagge E, Böhm E, Fritze R, Roose U J, Samorski M, Schnier C, Staubert R, Thielheim K O, Trümper J, Wiedecke L and Wolter W 1965 *Proc. 9th Int. Conf. on Cosmic Rays, London* vol 2 (London: The Institute of Physics and The Physical Society) pp 738–41

Bradt H V and Rappaport S A 1967 *Phys. Rev.* **164** 1567–83

Capdevielle J N 1972 *PhD Thesis* Université de Paris-Sud

Chatterjee B K, Murthy G T, Naranan S, Sreekantan B V, Srinivasa Rao M V, Tonwar S C and Vatcha R H 1968 *Can. J. Phys.* **46** 136–41

Dovzenko O J, Zatcepin G T, Murzina E A, Nikolskij S I and Iakovlev V I 1959 *Proc. 6th Int. Conf. on Cosmic Rays, Moscow* vol 2 134–41

Feinberg E L 1972 *Phys. Rep.* C **5** 237–350

Fritze R, Samorski M, Staubert R, Trümper J, Aschenbach B and Böhm E 1970 *Acta Phys. Hung.* **29** *Suppl.* 3 415–6

Hasegawa H, Noma M, Suga K and Toyoda Y 1965 *Proc. 9th Int. Conf. on Cosmic Rays, London* vol 2 (London: The Institute of Physics and The Physical Society) pp 642–5

Miyake S, Hinotani K, Ito N, Kino S, Sakuyama H, Kawakami S and Hayashida N 1970 *Acta. Phys. Hung.* **29** *Suppl.* 3 463–9

Murthy G T, Sivaprasad K, Srinivasa Rao M V, Tonwar S C, Vatcha R H and Viswanath P R 1968 *Can. J. Phys.* **46** 159–63

Murzin V S 1967 *Progress in Elementary Particle and Cosmic Ray Physics* vol 9, ed J G Wilson and S A Wouthuysen (Amsterdam: North-Holland) pp 247–303

Pinkau K 1965 *Phys. Rev.* **139** B1548–55

Rossi B 1952 *High Energy Particles* (New York: Prentice-Hall)

Samorski M 1973 *Nucl. Instrum. Meth.* **108** 285–9

Sreekantan B V 1971 *Proc. 12th Int. Conf. on Cosmic Rays, Hobart* vol 7 (Hobart: University of Tasmania) pp 2706–19

van Staa R, Aschenbach B, Böhm E and Cachon A 1973 *Proc. 13th Int. Conf. on Cosmic Rays, Denver* vol 4 pp 2676–81

Tanahashi G 1965 *J. Phys. Soc. Japan* **20** 883–906

Thielheim K O and Beiersdorf R 1969 *J. Phys.* A: *Gen. Phys.* **2** 341–53

Toyoda Y 1962 *J. Phys. Soc. Japan* **17** 415–26

Trümper J 1967 *Fortschr. Phys.* **15** 197–268

Yoshii H 1971 *J. Phys. Soc. Japan* **32** 295–305